Supplementary Text:
Emergenet: Fast Scalable Pandemic Risk Estimation of Influenza A Strains Collected In Non-human Hosts

Kevin Wu[1], Jin Li[1], Timmy Li[1], Aaron Esser-Kahn[2,3], and Ishanu Chattopadhyay[1,4,5]★

[1]Department of Medicine, University of Chicago, IL, USA
[2]Pritzker School of Molecular Engineering, University of Chicago, Chicago, IL, USA
[3]Committee on Immunology, University of Chicago, Chicago, IL, USA
[4]Committee on Genetics, Genomics & Systems Biology, University of Chicago, IL, USA
[5]Committee on Quantitative Methods in Social, Behavioral, and Health Sciences, University of Chicago, IL, USA

★To whom correspondence should be addressed: e-mail: ishanu@uchicago.edu.

SUPPLEMENTARY METHODS: NOTES ON Q-DISTANCE & SUPPORTING RESULTS

The *q-distance* is a pseudo-metric since distinct sequences can induce the same distributions over each index, and thus evaluate to have a zero distance. This is actually desirable; we do not want our distance to be sensitive to changes that are not biologically relevant. The intuition is that not all sequence variations brought about by substitutions are equally important or likely. Even with no selection pressure, we might still see random variations at an index if such variations do not affect the replicative fitness. Under that scenario, the corresponding Φ_i will predict a flat distribution no matter what the input sequence is, thus contributing nothing to the overall distance. And even if two strains x, y have the same entry at some index i, the remaining residues might induce different distributions Φ_i based on the remote dependencies, *i.e.*, the entries in x_{-i}, y_{-i}. Also, it matters if the sequences come from two different background populations P, Q, *i.e.*, if the induced Qnets Φ^P, Φ^Q are different. Thus, if we construct Qnets for H1N1 Influenza A separately for the collection years 2008 and 2009, then the same exact sequence collected in the respective years might have a non-zero distance between them, reflecting the fact that the background population the sequences arose from are different, inducing possibly different expected mutational tendencies (See SI-Table **??**).

Next, we induce q-distance between a sequence and a population and between two populations.

Definition 1 (Pseudo-metric between populations)**.** *Using the notion of Hausdorff metric between sets:*

$$\forall x \in P, y \in Q,$$

$$\theta(x, Q) = \min_{y \in Q} \theta(x, y) \tag{1}$$

$$\theta(P, Q) = \max \left\{ \max_{x \in P} \theta(x, Q), \max_{y \in Q} \theta(y, P) \right\} \tag{2}$$

In-silico Corroboration of Qnet Constraints

We carry out in-silico experiments to corroborate that the constraints represented within an inferred Qnet are indeed reflective of the biology in play. We compare the results of simulated mutational perturbations to sequences from our databases (for which we have already constructed Qnets), and then use NCBI BLAST (https://blast.ncbi.nlm.nih.gov/Blast.cgi) to identify if our perturbed sequences match with existing sequences in the databases (See SI-Fig. 1). We find that in contrast to random variations, which rapidly diverge the trajectories, the Qnet constraints tend to produce smaller variance in the trajectories, maintain a high degree of match as we extend our trajectories, and produces matches closer in time to the collection time of the initial sequence — suggesting that the Qnet does indeed capture realistic constraints.

Significance Test for Population Membership

For our modeling to be reliable, we need a quantitative test of how well the Qnet represents the data. Here, we formulate an explicit membership test to ascertain if individual samples may indeed be generated by the Qnet with sufficiently high probability.

Definition 2 (Membership probability of a sequence)**.** *Given a population P inducing the Qnet Φ^P and a sequence x, we can compute the membership probability of x:*

$$\omega_x^P \triangleq Pr(x \in P) = \prod_{j=1}^{N} \left(\Phi_j^P(x_{-j})|_{x_j}\right) \tag{3}$$

x_j is the j^{th} entry in x, and is thus an element in the set Σ_j. Since we are mostly concerned with the case where Σ_j is a finite set, $\Phi_j^P(x_{-j})|_{x_j}$ is the entry in the probability mass function corresponding to the element of Σ_j which appears at the j^{th} index in sequence x.

We can carry out this calculation for a sequence x known to be in the population P as well, which allows us to define the membership degree ω_x^P.

Definition 3 (Membership degree)**.** *Let X be a random field representing a population P, ie.. $X = x$ is a randomly drawn sequence from P. Then the membership degree ω^P is a function of the random variable X:*

$$\omega^P(X) \triangleq \prod_{j=1}^{N} \left(\Phi_j^P(X_{-j})|_{X_j}\right) \tag{4}$$

Note that ω^P takes values in the unit interval $[0, 1]$, and the probability x is a member of the population P is $\omega^P(X = x)$, denoted briefly as ω_x^P or ω_x if P is clear from context.

Since $\omega^P(X)$ is a random variable, we can now compute sets of sequences that better represent the population P, and ones that are on the fringe. We can also evaluate using a pre-specified significance-level if a particular sequence is not from the population P, thus identifying if we need to recompute the predictors Φ, or split the base population. We can set up a hypothesis testing scenario to determine if sequences are indeed from a test population, as follows:

Given a population P, inducing a Qnet Φ^P, and a sequence x, we assume the null hypothesis is $x \notin P$. We reject the null hypothesis at a pre-specified significance α, if

$$Pr(\omega^P(X) \geqq \omega^P(X = x)) \leqq \alpha \tag{5}$$

The fraction of newly observed sequences that do not reject the null hypothesis can then be used as an estimate of the species-specific divergence in population characteristics.

Proof of Probability Bounds

Theorem 1 (Probability bound)**.** *Given a sequence x of length N that transitions to a strain $y \in Q$, we have the following bounds at significance level α.*

$$\omega_y^Q e^{\frac{\sqrt{8}N^2}{1-\alpha}\theta(x,y)} \geqq Pr(x \to y) \geqq \omega_y^Q e^{-\frac{\sqrt{8}N^2}{1-\alpha}\theta(x,y)} \tag{6}$$

where ω_y^Q is the membership probability of strain y in the target population Q (See Def. 2), and $\theta(x, y)$ is the q-distance between x, y (See Def. 2 in Qnet Framework).

Proof. Using Sanov's theorem[1] on large deviations, we conclude that the probability of spontaneous jump from strain $x \in P$ to strain $y \in Q$, with the possibility $P \neq Q$, is given by:

$$Pr(x \to y) = \prod_{i=1}^{N} \left(\Phi_i^P(x_{-i})|_{y_i}\right) \tag{7}$$

Writing the factors on the right hand side as:

$$\Phi_i^P(x_{-i})|_{y_i} = \Phi_i^Q(y_{-i})|_{y_i} \left(\frac{\Phi_i^P(x_{-i})|_{y_i}}{\Phi_i^Q(y_{-i})|_{y_i}}\right) \tag{8}$$

we note that $\Phi_i^P(x_{-i})$, $\Phi_i^Q(y_{-i})$ are distributions on the same index i, and hence:

$$|\Phi_i^P(x_{-i})_{y_i} - \Phi_i^Q(y_{-i})_{y_i}| \leqq \sum_{y_i \in \Sigma_i} |\Phi_i^P(x_{-i})_{y_i} - \Phi_i^Q(y_{-i})_{y_i}| \tag{9}$$

Using a standard refinement of Pinsker's inequality[2], and the relationship of Jensen-Shannon divergence with total variation, we get:

$$\theta_i \geqq \frac{1}{8}|\Phi_i^P(x_{-i})_{y_i} - \Phi_i^Q(y_{-i})_{y_i}|^2 \Rightarrow \left|1 - \frac{\Phi_i^Q(y_{-i})_{y_i}}{\Phi_i^P(x_{-i})_{y_i}}\right| \leqq \frac{1}{a_0}\sqrt{8\theta_i} \tag{10}$$

where a_0 is the smallest non-zero probability value of generating the entry at any index. We will see that this

parameter is related to statistical significance of our bounds. First, we can formulate a lower bound as follows:

$$\log\left(\prod_{i=1}^{N}\frac{\Phi_i^P(x_{-i})|_{y_i}}{\Phi_i^Q(y_{-i})|_{y_i}}\right)=\sum_i\log\left(\frac{\Phi_i^P(x_{-i})|_{y_i}}{\Phi_i^Q(y_{-i})|_{y_i}}\right)\geqq\sum_i\left(1-\frac{\Phi_i^Q(y_{-i})_{y_i}}{\Phi_i^P(x_{-i})_{y_i}}\right)\geqq\frac{\sqrt{8}}{a_0}\sum_i\theta_i^{1/2}=-\frac{\sqrt{8}N}{a_0}\theta \tag{11}$$

Similarly, the upper bound may be derived as:

$$\log\left(\prod_{i=1}^{N}\frac{\Phi_i^P(x_{-i})|_{y_i}}{\Phi_i^Q(y_{-i})|_{y_i}}\right)=\sum_i\log\left(\frac{\Phi_i^P(x_{-i})|_{y_i}}{\Phi_i^Q(y_{-i})|_{y_i}}\right)\leqq\sum_i\left(\frac{\Phi_i^Q(y_{-i})_{y_i}}{\Phi_i^P(x_{-i})_{y_i}}-1\right)\leqq\frac{\sqrt{8}N}{a_0}\theta \tag{12}$$

Combining Eqs. 11 and 12, we conclude:

$$\omega_y^Q e^{\frac{\sqrt{8}N}{a_0}\theta}\geqq Pr(x\to y)\geqq\omega_y^Q e^{-\frac{\sqrt{8}N}{a_0}\theta} \tag{13}$$

Now, interpreting a_0 as the probability of generating an unlikely event below our desired threshold ($i.e.$ a "failure"), we note that the probability of generating at least one such event is given by $1-(1-a_0)^N$. Hence if α is the pre-specified significance level, we have for $N>>1$:

$$a_0\approx(1-\alpha)/N \tag{14}$$

Hence, we conclude, that at significance level $\geqq\alpha$, we have the bounds:

$$\omega_y^Q e^{\frac{\sqrt{8}N^2}{1-\alpha}\theta}\geqq Pr(x\to y)\geqq\omega_y^Q e^{-\frac{\sqrt{8}N^2}{1-\alpha}\theta} \tag{15}$$

□

Remark 1. *This bound can be rewritten in terms of the log-likelihood of the spontaneous jump and constants independent of the initial sequence x as:*

$$|\log Pr(x\to y)-C_0|\leqq C_1\theta \tag{16}$$

where the constants are given by:

$$C_0=\log\omega_y^Q \tag{17}$$

$$C_1=\frac{\sqrt{8}N^2}{1-\alpha} \tag{18}$$

Multivariate Regression to Identify Factors in Strain Prediction

We investigate the key factors that contribute to our successful prediction of the dominant strain in the next season. We carry out a multivariate regression with data diversity, the complexity of inferred Qnet and the edit distance of the WHO recommendation from the dominant strain as independent variables. Here we define data diversity as the number of clusters we have in the input set of sequences, such that any two sequences five or less mutations apart are in the same cluster. Qnet complexity is measured by the number of decision nodes in the component decision trees of the recursive forest.

We select several plausible structures of the regression equation, and in each case conclude that data diversity has the most important and statistically significant contribution (See SI-Tab. 12).

REFERENCES

[1] Cover TM, Thomas JA. Elements of Information Theory (Wiley Series in Telecommunications and Signal Processing). New York, NY, USA: Wiley-Interscience; 2006.

[2] Fedotov AA, Harremoës P, Topsoe F. Refinements of Pinsker's inequality. IEEE Transactions on Information Theory. 2003;49(6):1491–1498.

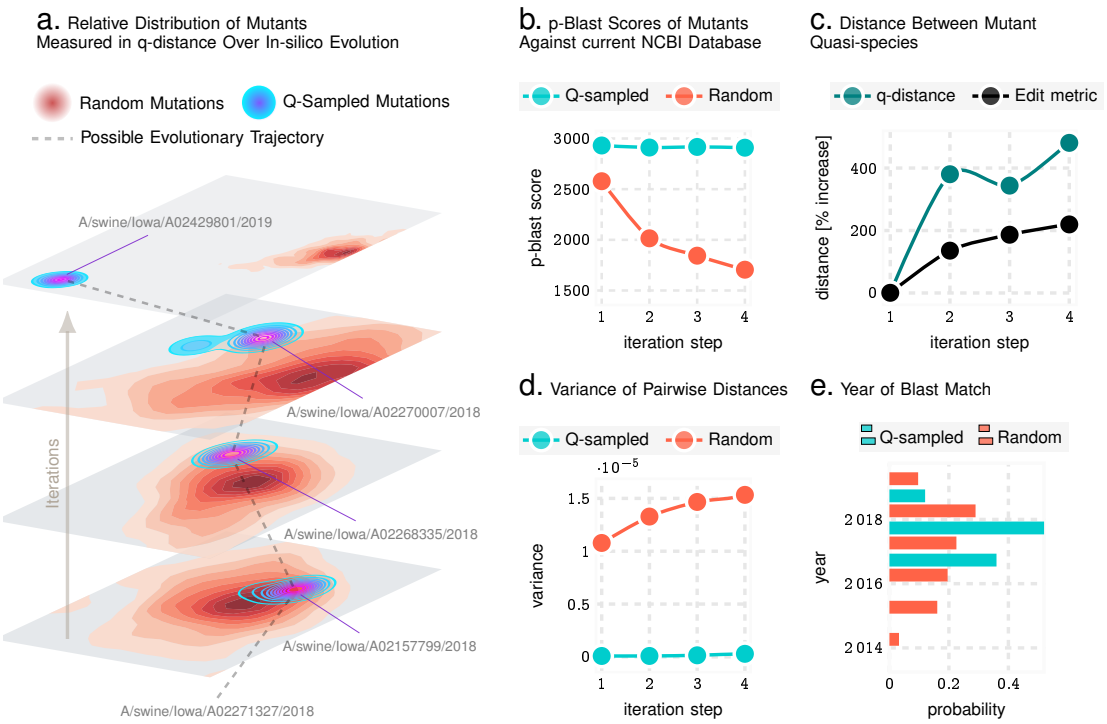

SI Fig. 1. **Q-distance validation in-silico using Influenza A sequences from NCBI database. Panel a** illustrates that the Qnet induced modeling of evolutionary trajectories initiated from known haemagglutinnin (HA) sequences are distinct from random paths in the strain space. In particular, random trajectories have more variance, and more importantly, diverge to different regions of the landscape compared to Qnet predictions. **Panels b-e** show that unconstrained Q-sampling produces sequences maintain a higher degree of similarity to known sequences, as verified by blasting against known HA sequences, have a smaller rate of growth of variance, and produce matches in closer time frames to the initial sequence. **Panel c** shows that this is not due to simply restricting the mutational variations, which increases rapidly in both the Qnet and the classical metric.

Supplementary Figures & Tables

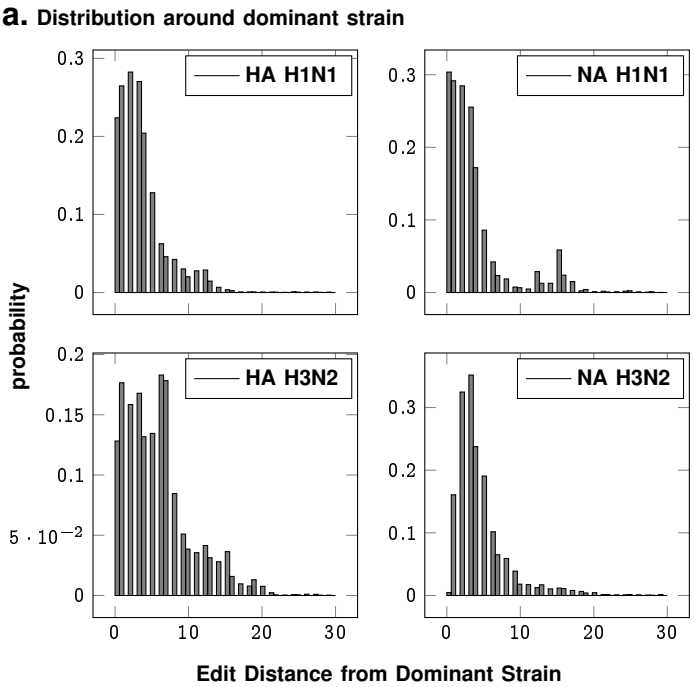

SI Fig. 2. **No. of mutations from the seasonal dominant strain over the years** The quasispecies that circulates each season for each sub-type is tightly distributed around the dominant strain on average.

SI Tab. 1
H1N1 NA NORTHERN HEMISPHERE

Year	WHO Recommendation	Dominant Strain	Qnet Recommendation	WHO Error	Qnet Error
2001-02	A/New Caledonia/20/99	A/New York/447/2001	A/Memphis/15/2000	4	4
2002-03	A/New Caledonia/20/99	A/Paris/0833/2002	A/New York/341/2001	1	5
2003-04	A/New Caledonia/20/99	A/Memphis/5/2003	A/New York/291/2002	3	5
2004-05	A/New Caledonia/20/99	A/Singapore/14/2004	A/New York/223/2003	2	3
2005-06	A/New Caledonia/20/99	A/Taiwan/5524/2005	A/Florida/3e/2004	3	0
2006-07	A/New Caledonia/20/99	A/Massachusetts/08/2006	A/Sofia/361/2005	4	2
2007-08	A/Solomon Islands/3/2006	A/Tennessee/UR06-0106/2007	A/Sofia/490/2006	9	2
2008-09	A/Brisbane/59/2007	A/Sendai/TU66/2008	A/Maryland/04/2007	0	3
2009-10	A/Brisbane/59/2007	A/Thailand/SR08021/2009	A/Paris/910/2008	87	87
2010-11	A/California/7/2009	A/Finland/2460N/2010	A/Rome/709/2009	2	9
2011-12	A/California/7/2009	A/Tula/CRIE-GSYu/2011	A/Oman/SQUH-40/2010	4	2
2012-13	A/California/7/2009	A/Bangalore/697-32/2012	A/Nizhnii Novgorod/CRIE-ZCA/2011	4	0
2013-14	A/California/7/2009	A/Jiangsugusu/SWL1824/2013	A/LongYan/SWL33/2013	5	3
2014-15	A/California/7/2009	A/LongYan/SWL2457/2014	A/Utah/06/2013	9	3
2015-16	A/California/7/2009	A/Michigan/45/2015	A/Maryland/02/2014	14	4
2016-17	A/California/7/2009	A/Mexico/4436/2016	A/India/Pun151245/2015	14	0
2017-18	A/Michigan/45/2015	A/Illinois/37/2017	A/Utah/02/2016	3	3
2018-19	A/Michigan/45/2015	A/Kenya/47/2018	A/Maine/24/2017	4	0
2019-20	A/Brisbane/02/2018	A/Texas/7939/2019	A/Missouri/03/2018	1	0
2020-21	A/Hawaii/70/2019	A/Togo/897/2020	A/Texas/112/2019	0	5
2021-22	A/Victoria/2570/2019	A/Cote_d'Ivoire/3729/2021	A/Togo/0071/2021	1	5
2022-23	-1	-1	A/Lyon/820/2021	-1	-1

* Dominant strain is calculated as the one closest to the centroid in the strain space that year in the edit distance metric

SI Tab. 2
H1N1 NA SOUTHERN HEMISPHERE

Year	WHO Recommendation	Dominant Strain	Qnet Recommendation	WHO Error	Qnet Error
2001-02	A/New Caledonia/20/99	A/New York/447/2001	A/Canterbury/37/2000	4	6
2002-03	A/New Caledonia/20/99	A/Paris/0833/2002	A/New York/447/2001	1	5
2003-04	A/New Caledonia/20/99	A/Memphis/5/2003	A/New York/291/2002	3	5
2004-05	A/New Caledonia/20/99	A/Singapore/14/2004	A/Memphis/5/2003	2	3
2005-06	A/New Caledonia/20/99	A/Taiwan/5524/2005	A/Canterbury/106/2004	3	6
2006-07	A/New Caledonia/20/99	A/Massachusetts/08/2006	A/Sofia/361/2005	4	2
2007-08	A/New Caledonia/20/99	A/Tennessee/UR06-0106/2007	A/Thailand/RMSC-UDN-20/2006	4	8
2008-09	A/Solomon Islands/3/2006	A/Sendai/TU66/2008	A/Tennessee/UR06-0151/2007	15	13
2009-10	A/Brisbane/59/2007	A/Thailand/SR08021/2009	A/Nebraska/07/2008	87	87
2010-11	A/California/7/2009	A/Finland/2460N/2010	A/Rome/709/2009	2	9
2011-12	A/California/7/2009	A/Tula/CRIE-GSYu/2011	A/Finland/2460N/2010	4	2
2012-13	A/California/7/2009	A/Bangalore/697-32/2012	A/Tula/CRIE-GSYu/2011	4	0
2013-14	A/California/7/2009	A/Jiangsugusu/SWL1824/2013	A/Oman/SQUH-63/2012	5	4
2014-15	A/California/7/2009	A/LongYan/SWL2457/2014	A/NanPing/SWL1640/2013	9	6
2015-16	A/California/7/2009	A/Michigan/45/2015	A/LongYan/SWL2457/2014	14	5
2016-17	A/California/7/2009	A/Mexico/4436/2016	A/Michigan/45/2015	14	0
2017-18	A/Michigan/45/2015	A/Illinois/37/2017	A/Mexico/4436/2016	3	3
2018-19	A/Michigan/45/2015	A/Kenya/47/2018	A/Kentucky/26/2017	4	2
2019-20	A/Michigan/45/2015	A/Texas/7939/2019	A/Kenya/47/2018	4	0
2020-21	A/Brisbane/02/2018	A/Togo/897/2020	A/Texas/7939/2019	6	5
2021-22	A/Victoria/2570/2019	A/Cote_D'Ivoire/1496/2021	A/NAGASAKI/8/2020	1	6
2022-23	-1	-1	A/Dakar/35/2021	-1	-1

* Dominant strain is calculated as the one closest to the centroid in the strain space that year in the edit distance metric

SI Tab. 3
H3N2 NA NORTHERN HEMISPHERE

Year	WHO Recommendation	Dominant Strain	Qnet Recommendation	WHO Error	Qnet Error
2003-04	A/Moscow/10/99	A/Denmark/107/2003	A/New York/100/2002	13	3
2004-05	A/Fujian/411/2002	A/Hyogo/36/2004	A/New York/20/2003	3	16
2005-06	A/California/7/2004	A/Denmark/203/2005	A/Hong Kong/HKU20/2004	4	0
2006-07	A/Wisconsin/67/2005	A/Berlin/32/2006	A/Mexico/InDRE2227/2005	1	1
2007-08	A/Wisconsin/67/2005	A/Brazil/80/2007	A/Baden-Wuerttemberg/17/2006	8	7
2008-09	A/Brisbane/10/2007	A/Missouri/05/2008	A/Washington/01/2007	3	2
2009-10	A/Brisbane/10/2007	A/Oklahoma/09/2009	A/Wisconsin/24/2008	3	1
2010-11	A/Perth/16/2009	A/California/17/2010	A/New York/70/2009	2	3
2011-12	A/Perth/16/2009	A/Texas/14/2011	A/California/14/2010	3	2
2012-13	A/Victoria/361/2011	A/New York/02/2012	A/Singapore/C2011.493/2011	4	1
2013-14	A/Victoria/361/2011	A/Michigan/02/2013	A/New York/01/2012	3	1
2014-15	A/Texas/50/2012	A/Tehran/69634/2014	A/Boston/DOA2-176/2013	3	1
2015-16	A/Switzerland/9715293/2013	A/Parma/471/2015	A/Thailand/CU-B10520/2014	3	0
2016-17	A/Hong Kong/4801/2014	A/North Carolina/62/2016	A/Delaware/02/2015	7	2
2017-18	A/Hong Kong/4801/2014	A/Texas/277/2017	A/New York/03/2016	8	0
2018-19	A/Singapore/INFIMH-16-0019/2016	A/Japan/NHRC_FDX70352/2018	A/Colorado/11/2017	4	3
2019-20	A/Kansas/14/2017	A/Washington/9757/2019	A/Guangxi-Fangcheng/54/2019	3	11
2020-21	A/Hong Kong/2671/2019	A/Bangladesh/1004005/2020	A/Maryland/02/2019	3	13
2021-22	A/Cambodia/e0826360/2020	A/Stockholm/10/2022	A/Bangladesh/1916/2020	2	2
2022-23	-1	-1	A/Iowa/20/2022	-1	-1

* Dominant strain is calculated as the one closest to the centroid in the strain space that year in the edit distance metric

SI Tab. 4
H3N2 NA SOUTHERN HEMISPHERE

Year	WHO Recommendation	Dominant Strain	Qnet Recommendation	WHO Error	Qnet Error
2003-04	A/Moscow/10/99	A/Denmark/107/2003	A/New York/101/2002	13	3
2004-05	A/Fujian/411/2002	A/Hyogo/36/2004	A/New York/20/2003	3	16
2005-06	A/Wellington/1/2004	A/Denmark/203/2005	A/Wellington/1/2004	2	2
2006-07	A/California/7/2004	A/Berlin/32/2006	A/Mexico/InDRE2227/2005	3	1
2007-08	A/Wisconsin/67/2005	A/Brazil/80/2007	A/Ohio/06/2006	8	10
2008-09	A/Brisbane/10/2007	A/Missouri/05/2008	A/Brazil/80/2007	3	2
2009-10	A/Brisbane/10/2007	A/Oklahoma/09/2009	A/Wisconsin/24/2008	3	1
2010-11	A/Perth/16/2009	A/California/17/2010	A/New York/70/2009	2	3
2011-12	A/Perth/16/2009	A/Texas/14/2011	A/Virginia/05/2010	3	2
2012-13	A/Perth/16/2009	A/New York/02/2012	A/Texas/14/2011	4	1
2013-14	A/Victoria/361/2011	A/Michigan/02/2013	A/New York/02/2012	3	3
2014-15	A/Texas/50/2012	A/Tehran/69634/2014	A/Michigan/02/2013	3	1
2015-16	A/Switzerland/9715293/2013	A/Parma/471/2015	A/Tehran/69634/2014	3	2
2016-17	A/Hong Kong/4801/2014	A/North Carolina/62/2016	A/Parma/471/2015	7	2
2017-18	A/Hong Kong/4801/2014	A/Texas/277/2017	A/Guangdong/264/2016	8	0
2018-19	A/Singapore/INFIMH-16-0019/2016	A/Japan/NHRC_FDX70352/2018	A/Texas/277/2017	4	3
2019-20	A/Switzerland/8060/2017	A/Washington/9757/2019	A/Pennsylvania/317/2018	10	10
2020-21	A/South Australia/34/2019	A/Bangladesh/1004005/2020	A/Washington/9757/2019	1	13
2021-22	A/Hong Kong/2671/2019	A/India/PUN-NIV301718/2021	A/India/PUN-NIV301132/2021	6	4
2022-23	-1	-1	A/Michigan/UOM10045036720/2022	-1	-1

* Dominant strain is calculated as the one closest to the centroid in the strain space that year in the edit distance metric

SI Tab. 5
H1N1 NA NORTHERN HEMISPHERE (MULTI-CLUSTER)

Year	WHO Recommendation	WHO Error	Qnet Error 1	Qnet Error 2	Qnet Recommendation 1	Qnet Recommendation 2
2001-02	A/New Caledonia/20/99	4	1	6	A/New South Wales/26/2000	A/Canterbury/37/2000
2002-03	A/New Caledonia/20/99	1	0	5	A/Wellington/1/2001	A/New York/447/2001
2003-04	A/New Caledonia/20/99	3	2	8	A/Paris/0833/2002	A/Taiwan/141/2002
2004-05	A/New Caledonia/20/99	2	3	4	A/Memphis/5/2003	A/Hanoi/1004/2003
2005-06	A/New Caledonia/20/99	3	0	1	A/Denmark/130/2004	A/Paris/650/2004
2006-07	A/New Caledonia/20/99	4	2	8	A/Sofia/361/2005	A/Wellington/11/2005
2007-08	A/Solomon Islands/3/2006	9	4	8	A/Sofia/246/2006	A/New York/8/2006
2008-09	A/Brisbane/59/2007	0	13	19	A/Tennessee/UR06-0151/2007	A/Ohio/UR06-0178/2007
2009-10	A/Brisbane/59/2007	87	88	90	A/Sendai/TU66/2008	A/Japan/618/2008
2010-11	A/California/7/2009	2	1	6	A/South Carolina/WRAIR1645P/2009	A/Wisconsin/629-D00809/2009
2011-12	A/California/7/2009	4	1	3	A/England/21680633/2010	A/Hangzhou/178/2010
2012-13	A/California/7/2009	4	1	22	A/Joshkar-Ola/CRIE-BLP/2011	A/Rio Grande do Sul/578/2011
2013-14	A/California/7/2009	5	4	13	A/Thailand/MR10580/2012	A/Mexico/INMEGEN-INER 15/2012
2014-15	A/California/7/2009	9	3	7	A/Minnesota/02/2013	A/Helsinki/430/2013
2015-16	A/California/7/2009	14	4	7	A/Helsinki/808M/2014	A/Virginia/NHRC430739/2014
2016-17	A/California/7/2009	14	0	3	A/Michigan/45/2015	A/Colorado/30/2015
2017-18	A/Michigan/45/2015	3	3	8	A/Mexico/4436/2016	A/Arizona/03/2016
2018-19	A/Michigan/45/2015	4	0	4	A/California/NHRC_QV11073/2017	A/Minnesota/35/2017
2019-20	A/Brisbane/02/2018	1	0	2	A/Kenya/47/2018	A/Colorado/7682/2018
2020-21	A/Hawaii/70/2019	0	3	8	A/California/NHRC-OID_BOX-ILI-0012/2019	A/Indiana/30/2019
2021-22	A/Victoria/2570/2019	1	5	51	A/Togo/0071/2021	A/Yunnan-Mengzi/1462/2020
2022-23	-1	-1	-1	-1	A/Netherlands/10646/2022	A/Sydney/234/2022

* Dominant strain is calculated as the one closest to the centroid in the strain space that year in the edit distance metric

SI Tab. 6
H1N1 NA SOUTHERN HEMISPHERE (MULTI-CLUSTER)

Year	WHO Recommendation	WHO Error	Qnet Error 1	Qnet Error 2	Qnet Recommendation 1	Qnet Recommendation 2
2001-02	A/New Caledonia/20/99	4	1	6	A/New South Wales/26/2000	A/Canterbury/37/2000
2002-03	A/New Caledonia/20/99	1	0	5	A/Wellington/1/2001	A/New York/447/2001
2003-04	A/New Caledonia/20/99	3	2	8	A/Paris/0833/2002	A/Taiwan/141/2002
2004-05	A/New Caledonia/20/99	2	3	4	A/Memphis/5/2003	A/Hanoi/1004/2003
2005-06	A/New Caledonia/20/99	3	0	1	A/Denmark/130/2004	A/Paris/650/2004
2006-07	A/New Caledonia/20/99	4	2	8	A/Sofia/361/2005	A/Wellington/11/2005
2007-08	A/New Caledonia/20/99	4	4	8	A/Sofia/246/2006	A/New York/8/2006
2008-09	A/Solomon Islands/3/2006	15	13	19	A/Tennessee/UR06-0151/2007	A/Ohio/UR06-0178/2007
2009-10	A/Brisbane/59/2007	87	88	90	A/Sendai/TU66/2008	A/Japan/618/2008
2010-11	A/California/7/2009	2	1	6	A/South Carolina/WRAIR1645P/2009	A/Wisconsin/629-D00809/2009
2011-12	A/California/7/2009	4	1	3	A/England/21680633/2010	A/Hangzhou/178/2010
2012-13	A/California/7/2009	4	1	22	A/Joshkar-Ola/CRIE-BLP/2011	A/Rio Grande do Sul/578/2011
2013-14	A/California/7/2009	5	4	13	A/Thailand/MR10580/2012	A/Mexico/INMEGEN-INER 15/2012
2014-15	A/California/7/2009	9	3	7	A/Minnesota/02/2013	A/Helsinki/430/2013
2015-16	A/California/7/2009	14	4	7	A/Helsinki/808M/2014	A/Virginia/NHRC430739/2014
2016-17	A/California/7/2009	14	0	3	A/Michigan/45/2015	A/Colorado/30/2015
2017-18	A/Michigan/45/2015	3	3	8	A/Mexico/4436/2016	A/Arizona/03/2016
2018-19	A/Michigan/45/2015	4	0	4	A/California/NHRC_QV11073/2017	A/Minnesota/35/2017
2019-20	A/Michigan/45/2015	4	0	2	A/Kenya/47/2018	A/Colorado/7682/2018
2020-21	A/Brisbane/02/2018	5	2	7	A/California/NHRC-OID_BOX-ILI-0012/2019	A/Indiana/30/2019
2021-22	A/Victoria/2570/2019	1	7	58	A/Togo/0155/2021	A/Shandong/00204/2021
2022-23	-1	-1	-1	-1	A/Switzerland/86136/2022	A/Wisconsin/04/2021

* Dominant strain is calculated as the one closest to the centroid in the strain space that year in the edit distance metric

SI Tab. 7
H3N2 NA NORTHERN HEMISPHERE (MULTI-CLUSTER)

Year	WHO Recommendation	WHO Error	Qnet Error 1	Qnet Error 2	Qnet Recommendation 1	Qnet Recommendation 2
2003-04	A/Moscow/10/99	13	4	5	A/Auckland/612/2002	A/New York/87/2002
2004-05	A/Fujian/411/2002	3	16	18	A/New York/20/2003	A/New York/12/2003
2005-06	A/California/7/2004	4	1	7	A/New York/358/2004	A/Singapore/36/2004
2006-07	A/Wisconsin/67/2005	1	3	8	A/Macau/557/2005	A/Hong Kong/HKU53/2005
2007-08	A/Wisconsin/67/2005	8	0	10	A/Wisconsin/42/2006	A/Wisconsin/44/2006
2008-09	A/Brisbane/10/2007	3	4	10	A/Missouri/06/2007	A/Japan/72/2007
2009-10	A/Brisbane/10/2007	3	1	7	A/Wisconsin/24/2008	A/Mississippi/UR07-0042/2008
2010-11	A/Perth/16/2009	2	3	8	A/New York/70/2009	A/Japan/883/2009
2011-12	A/Perth/16/2009	3	2	2	A/California/19/2010	A/Virginia/05/2010
2012-13	A/Victoria/361/2011	4	1	12	A/Texas/14/2011	A/Singapore/GP1684/2011
2013-14	A/Victoria/361/2011	3	1	5	A/Idaho/38/2012	A/Pavia/135/2012
2014-15	A/Texas/50/2012	3	1	1	A/Nevada/05/2013	A/Michigan/02/2013
2015-16	A/Switzerland/9715293/2013	3	0	4	A/Nicaragua/6866_14/2014	A/Iran/91244/2014
2016-17	A/Hong Kong/4801/2014	7	1	25	A/New Jersey/13/2015	A/California/NHRC_BRD41056N/2015
2017-18	A/Hong Kong/4801/2014	9	1	4	A/Guangdong/264/2016	A/Victoria/668/2016
2018-19	A/Singapore/INFIMH-16-0019/2016	3	2	4	A/Netherlands/3530/2017	A/Washington/17/2017
2019-20	A/Kansas/14/2017	3	4	10	A/England/538/2018	A/California/BRD12490N/2018
2020-21	A/Hong Kong/2671/2019	3	1	13	A/England/9738/2019	A/Washington/9757/2019
2021-22	A/Cambodia/e0826360/2020	2	3	7	A/Laos/527/2021	A/Michigan/UOM10045655748/2020
2022-23	-1	-1	-1	-1	A/Maine/02/2022	A/Michigan/UOM10042819294/2021

* Dominant strain is calculated as the one closest to the centroid in the strain space that year in the edit distance metric

SI Tab. 8
H3N2 NA SOUTHERN HEMISPHERE (MULTI-CLUSTER)

Year	WHO Recommendation	WHO Error	Qnet Error 1	Qnet Error 2	Qnet Recommendation 1	Qnet Recommendation 2
2003-04	A/Moscow/10/99	13	4	5	A/Auckland/612/2002	A/New York/87/2002
2004-05	A/Fujian/411/2002	3	16	18	A/New York/20/2003	A/New York/12/2003
2005-06	A/Wellington/1/2004	2	1	7	A/New York/358/2004	A/Singapore/36/2004
2006-07	A/California/7/2004	3	3	8	A/Macau/557/2005	A/Hong Kong/HKU53/2005
2007-08	A/Wisconsin/67/2005	8	0	10	A/Wisconsin/42/2006	A/Wisconsin/44/2006
2008-09	A/Brisbane/10/2007	3	4	10	A/Missouri/06/2007	A/Japan/72/2007
2009-10	A/Brisbane/10/2007	3	1	7	A/Wisconsin/24/2008	A/Mississippi/UR07-0042/2008
2010-11	A/Perth/16/2009	2	3	8	A/New York/70/2009	A/Japan/883/2009
2011-12	A/Perth/16/2009	3	2	2	A/California/19/2010	A/Virginia/05/2010
2012-13	A/Perth/16/2009	4	1	12	A/Texas/14/2011	A/Singapore/GP1684/2011
2013-14	A/Victoria/361/2011	3	1	5	A/Idaho/38/2012	A/Pavia/135/2012
2014-15	A/Texas/50/2012	3	1	1	A/Nevada/05/2013	A/Michigan/02/2013
2015-16	A/Switzerland/9715293/2013	3	0	4	A/Nicaragua/6866_14/2014	A/Iran/91244/2014
2016-17	A/Hong Kong/4801/2014	7	1	25	A/New Jersey/13/2015	A/California/NHRC_BRD41056N/2015
2017-18	A/Hong Kong/4801/2014	9	1	4	A/Guangdong/264/2016	A/Victoria/668/2016
2018-19	A/Singapore/INFIMH-16-0019/2016	3	2	4	A/Netherlands/3530/2017	A/Washington/17/2017
2019-20	A/Switzerland/8060/2017	10	4	10	A/England/538/2018	A/California/BRD12490N/2018
2020-21	A/South Australia/34/2019	1	1	13	A/England/9738/2019	A/Washington/9757/2019
2021-22	A/Hong Kong/2671/2019	6	1	49	A/Darwin/11/2021	A/Hawaii/28/2020
2022-23	-1	-1	-1	-1	A/Congo/313/2021	A/Texas/12723/2022

* Dominant strain is calculated as the one closest to the centroid in the strain space that year in the edit distance metric

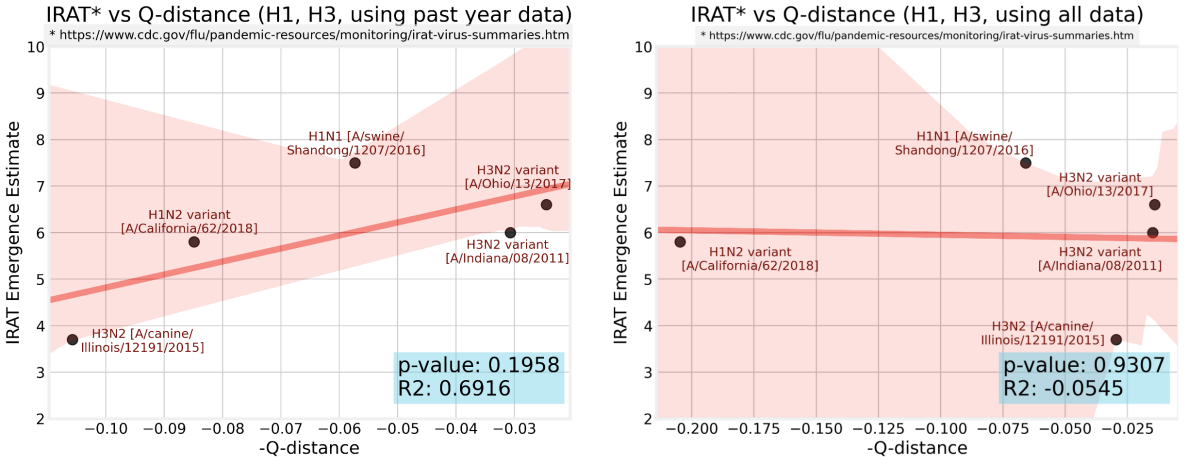

SI Fig. 3. **IRAT vs. Q-distance relationship for H1- and H3- sub-types, using past year data vs. using all data.** On the result when computing average q-distance between the target strain and the circulating human strains from the past year, and on the right is the result when using all available human strains of that sub-type. Evidently, the former has a much higher correlation, since a strain being “close” to humans at some point does not necessarily mean being close now.

SI Tab. 9
INFLUENZA A STRAINS EVALUATED BY IRAT AND CORRESPONDING QNET COMPUTED RISK SCORES

Influenza Virus	Subype	IRAT Date	IRAT Emergence Score	IRAT Impact Score	HA Qnet Sample	NA Qnet Sample	HA Avg. Q-dist.	NA Avg. Q-dist.	Geom. Mean	Qnet Emergence Score	Qnet Impact Score
A/swine/Shandong/1207/2016	H1N1	Jul 2020	7.5	6.9	1000	1000	0.0941	0.0205	0.0440	6.0	6.2
A/Ohio/13/2017	H3N2	Jul 2019	6.6	5.8	1000	1000	0.0184	0.0306	0.0238	6.3	6.2
A/Hong Kong/125/2017	H7N9	May 2017	6.5	7.5	437	437	0.0296	0.0058	0.0131	6.6	6.5
A/Shanghai/02/2013	H7N9	Apr 2016	6.4	7.2	178	178	0.0055	0.0036	0.0044	6.7	6.6
A/Anhui-Lujiang/39/2018	H9N2	Jul 2019	6.2	5.9	31	30	0.0290	0.1681	0.0698	5.2	5.0
A/Indiana/08/2011	H3N2	Dec 2012	6.0	4.5	1000	1000	0.0523	0.0091	0.0218	6.4	6.5
A/California/62/2018	H1N2	Jul 2019	5.8	5.7	55	55	0.1089	0.0610	0.0815	5.4	5.5
A/Bangladesh/0994/2011***	H9N2	Feb 2014	5.6	5.4	-1	-1	0.2078	0.1823	0.1947	4.3	4.9
A/Sichuan/06681/2021	H5N6	Oct 2021	5.3	6.3	45	45	0.3616	0.0518	0.1369	5.2	6.4
A/Vietnam/1203/2004	H5N1	Nov 2011	5.2	6.6	258	246	0.1673	0.0111	0.0430	6.2	6.7
A/Yunnan/14564/2015**	H5N6	Apr 2016	5.0	6.6	344	331	0.3482	0.2987	0.3225	4.9	6.5
A/Astrakhan/3212/2020**	H5N8	Mar 2021	4.6	5.2	381	365	0.1603	0.3472	0.2359	3.9	4.4
A/Netherlands/219/2003	H7N7	Jun 2012	4.6	5.8	46	46	0.2757	0.3521	0.3115	4.6	5.8
A/American wigeon/South Carolina/AH0195145/2021	H5N1	Mar 2022	4.4	5.1	335	323	0.1722	0.5114	0.2967	4.0	4.7
A/Jiangxi-Donghu/346/2013***	H10N8	Feb 2014	4.3	6.0	-1	-1	0.2088	0.2101	0.2094	4.3	4.8
A/gyrfalcon/Washington/41088/2014**	H5N8	Mar 2015	4.2	4.6	341	328	0.1532	0.3424	0.2290	3.9	4.3
A/Northern pintail/Washington/40964/2014**	H5N2	Mar 2015	3.8	4.1	341	328	0.1529	0.3799	0.2410	3.9	4.3
A/canine/Illinois/12191/2015	H3N2	Jun 2016	3.7	3.7	1000	1000	0.0607	0.1509	0.0957	4.9	4.8
A/American green-winged teal /Washington/1957050/2014	H5N1	Mar 2015	3.6	4.1	326	314	0.1911	0.4482	0.2927	4.1	4.9
A/turkey/Indiana/1573-2/2016**	H7N8	Jul 2017	3.4	3.9	495	494	0.1130	0.7738	0.2957	3.4	3.9
A/chicken/Tennessee/17-007431-3/2017	H7N9	Oct 2017	3.1	3.5	496	495	0.1027	0.2569	0.1624	4.1	4.2
A/chicken/Tennessee/17-007147-2/2017	H7N9	Oct 2017	2.8	3.5	496	495	0.2095	0.2541	0.2307	4.2	4.8
A/duck/New York/1996 *	H1N1	Nov 2011	2.3	2.4	1000	1000	-1	-1	-1	-1	-1

* HA strain is not available for A/duck/New York/1996, so this strain is omitted.
** Could not construct a Qnet of human sequence data available for that virus sub-type (less than 30 strains), so we constructed a Qnet using all human strains that match the HA sub-type, i.e. H5NX for H5N6.
*** These strains did not have enough human sequence data to generate a Qnet, even when only considering the HA sub-type. Thus, we estimated the risk score using every Qnet from the other IRAT strains, and took the average among NA and HA. Finally, we took the geometric mean of the resulting NA and HA averages.

SI Tab. 10
INFLUENZA A STRAINS EVALUATED BY IRAT AND CORRESPONDING QNET COMPUTED CURRENT RISK SCORES

Influenza Virus	Subype	IRAT Date	IRAT Emer-gence Score	IRAT Impact Score	HA Qnet Sample	NA Qnet Sample	HA Avg. Q-dist.	NA Avg. Q-dist.	Geom. Mean	Qnet Emer-gence Score	Qnet Impact Score
A/swine/Shandong/1207/2016	H1N1	Jul 2020	7.5	6.9	1000	1000	0.0599	0.0417	0.0500	5.8	5.8
A/Ohio/13/2017	H3N2	Jul 2019	6.6	5.8	1000	1000	0.0091	0.0692	0.0251	6.2	6.0
A/Hong Kong/125/2017	H7N9	May 2017	6.5	7.5	1000	1000	0.0092	0.0046	0.0065	6.7	6.6
A/Shanghai/02/2013	H7N9	Apr 2016	6.4	7.2	1000	1000	0.0031	0.0044	0.0037	6.8	6.6
A/Anhui-Lujiang/39/2018	H9N2	Jul 2019	6.2	5.9	58	58	0.0157	0.0467	0.0271	6.2	6.0
A/Indiana/08/2011	H3N2	Dec 2012	6.0	4.5	1000	1000	0.0176	0.0184	0.0180	6.4	6.3
A/California/62/2018	H1N2	Jul 2019	5.8	5.7	37	37	0.2038	0.0477	0.0986	5.3	5.9
A/Bangladesh/0994/2011	H9N2	Feb 2014	5.6	5.4	58	58	0.0473	0.4654	0.1484	3.8	3.6
A/Sichuan/06681/2021	H5N6	Oct 2021	5.3	6.3	46	46	0.3443	0.0600	0.1437	5.1	6.2
A/Vietnam/1203/2004	H5N1	Nov 2011	5.2	6.6	48	45	0.1323	0.0411	0.0738	5.6	5.8
A/Yunnan/14564/2015	H5N6	Apr 2016	5.0	6.6	46	46	0.2187	0.0415	0.0953	5.4	6.0
A/Astrakhan/3212/2020	H5N8	Mar 2021	4.6	5.2	95	92	0.2366	0.5451	0.3591	4.8	6.1
A/Netherlands/219/2003	H7N7	Jun 2012	4.6	5.8	1000	1000	0.1658	0.4596	0.2760	3.9	4.5
A/American wigeon/South Carolina/AH0195145/2021	H5N1	Mar 2022	4.4	5.1	48	45	0.2355	0.3135	0.2717	4.3	5.2
A/Jiangxi-Donghu/346/2013**	H10N8	Feb 2014	4.3	6.0	-1	-1	0.2097	0.2299	0.2196	4.2	4.8
A/gyrfalcon/Washington/ 41088/2014	H5N8	Mar 2015	4.2	4.6	95	92	0.2387	0.5438	0.3603	4.8	6.1
A/Northern pintail /Washington/40964/2014	H5N2	Mar 2015	3.8	4.1	95	92	0.2327	0.5099	0.3445	4.6	5.8
A/canine/Illinois/12191/2015	H3N2	Jun 2016	3.7	3.7	1000	1000	0.0179	0.0374	0.0259	6.2	6.1
A/American green-winged teal /Washington/1957050/2014	H5N1	Mar 2015	3.6	4.1	48	45	0.2352	0.3067	0.2686	4.3	5.1
A/turkey/Indiana/1573-2/2016	H7N8	Jul 2017	3.4	3.9	1000	1000	0.0438	0.4165	0.1351	4.0	3.8
A/chicken/Tennessee/17-007431-3/2017	H7N9	Oct 2017	3.1	3.5	1000	1000	0.0335	0.5127	0.1310	3.8	3.6
A/chicken/Tennessee/17-007147-2/2017	H7N9	Oct 2017	2.8	3.5	1000	1000	0.0839	0.5127	0.2075	3.5	3.6
A/duck/New York/1996*	H1N1	Nov 2011	2.3	2.4	1000	1000	-1	-1	-1	-1	-1

*This table contains Qnet scores for IRAT computed using current sequence data, thereby computing the current risk of these strains. -1 indicates missing data, either from lack of human sequence data available for that virus sub-type (less than 30 strains) or missing IRAT sequence data (in the case of A/duck/New York/1996)

SI Tab. 11
GENERAL LINEAR MODEL FOR EVALUATING EFFECT OF DATA DIVERSITY ON QNET PERFORMANCE

Variable Name	Description
qnet_complexity	Cumulative number of nodes in all predictors in the corresponding Qnet
data_diversity	Number of clusters in set of input sequence where each sequence in a specific cluster is separated by at least 5 mutations from sequences not in the cluster
ldistance_WHO	Deviation of WHO predicted strain from the dominant strain

```
model:dev ~ qnet_complexity + data_diversity + qnet_complexity * data_diversity + ldistance_WHO
                 Generalized Linear Model Regression Results
==============================================================================
Dep. Variable:                    dev   No. Observations:                  235
Model:                            GLM   Df Residuals:                      230
Model Family:                Gaussian   Df Model:                            4
Link Function:               identity   Scale:                          23.214
Method:                          IRLS   Log-Likelihood:                -700.43
Date:                Thu, 11 Jun 2020   Deviance:                       5339.2
Time:                        16:45:46   Pearson chi2:                 5.34e+03
No. Iterations:                     3   Covariance Type:             nonrobust
=========================================================================================================
                                     coef    std err          z      P>|z|      [0.025      0.975]
---------------------------------------------------------------------------------------------------------
Intercept                         -0.1116      1.090     -0.102      0.918      -2.248       2.025
qnet_complexity                    0.0005      0.000      1.075      0.282      -0.000       0.001
data_diversity                     0.3197      0.126      2.531      0.011       0.072       0.567
qnet_complexity:data_diversity -6.932e-05   5.01e-05     -1.383      0.167      -0.000    2.89e-05
ldistance_WHO                     -0.0348      0.035     -1.007      0.314      -0.102       0.033
=========================================================================================================


model:dev ~ qnet_complexity + data_diversity + ldistance_WHO
                 Generalized Linear Model Regression Results
==============================================================================
Dep. Variable:                    dev   No. Observations:                  235
Model:                            GLM   Df Residuals:                      231
Model Family:                Gaussian   Df Model:                            3
Link Function:               identity   Scale:                          23.306
Method:                          IRLS   Log-Likelihood:                -701.41
Date:                Thu, 11 Jun 2020   Deviance:                       5383.6
Time:                        16:45:47   Pearson chi2:                 5.38e+03
No. Iterations:                     3   Covariance Type:             nonrobust
==============================================================================
                     coef    std err          z      P>|z|      [0.025      0.975]
------------------------------------------------------------------------------
Intercept          1.0841      0.665      1.630      0.103      -0.219       2.387
qnet_complexity -4.12e-05      0.000     -0.156      0.876      -0.001       0.000
data_diversity     0.1788      0.075      2.392      0.017       0.032       0.325
ldistance_WHO     -0.0695      0.024     -2.930      0.003      -0.116      -0.023
==============================================================================
```

SI Tab. 12

GENERAL LINEAR MODEL EVALUATING QNET EMERGENCE RISK PREDICTIONS AGAINST IRAT ESTIMATES

Model: IRAT_Emergence_Score ~ Geometric_Mean

Dep. Variable:	IRAT_Emergence_Score	No. Observations:	22
Model:	GLM	Df Residuals:	20
Model Family:	Gaussian	Df Model:	1
Link Function:	identity	Scale:	0.86853
Method:	IRLS	Log-Likelihood:	-28.618
Date:	Tue, 25 Oct 2022	Deviance:	17.371
Time:	00:58:27	Pearson chi2:	17.4
No. Iterations:	3	Pseudo R-squ. (CS):	0.5919
Covariance Type:	nonrobust		

	coef	std err	z	P>|z|	[0.025	0.975]
Intercept	6.2467	0.356	17.529	0.000	5.548	6.945
Geometric_Mean	-8.1063	1.830	-4.429	0.000	-11.693	-4.519

Model: IRAT_Emergence_Score ~ Geometric_Mean + HA_Avg_Qdist*NA_Avg_Qdist

Dep. Variable:	IRAT_Emergence_Score	No. Observations:	22
Model:	GLM	Df Residuals:	17
Model Family:	Gaussian	Df Model:	4
Link Function:	identity	Scale:	0.69369
Method:	IRLS	Log-Likelihood:	-24.357
Date:	Tue, 25 Oct 2022	Deviance:	11.793
Time:	00:58:59	Pearson chi2:	11.8
No. Iterations:	3	Pseudo R-squ. (CS):	0.7797
Covariance Type:	nonrobust		

	coef	std err	z	P>|z|	[0.025	0.975]
Intercept	6.8403	0.442	15.459	0.000	5.973	7.708
Geometric_Mean	-23.7466	9.674	-2.455	0.014	-42.707	-4.786
HA_Avg_Qdist	1.9097	3.979	0.480	0.631	-5.889	9.708
NA_Avg_Qdist	-1.8133	2.826	-0.642	0.521	-7.353	3.726
HA_Avg_Qdist:NA_Avg_Qdist	54.2280	21.474	2.525	0.012	12.139	96.317

SI Tab. 13

NUMBERING CONVERSION TO PDM09 AND H3 SCHEMES

Query	H1N1pdm	H3
1	-	-
2	-	-
3	-	-
4	-	-
5	-	-
6	-	-
7	-	-
8	-	-
9	-	-
10	-	-
11	-	-
12	-	-
13	-	-
14	-	-
15	-	-
16	-	-
17	-	-
-	-	1
-	-	2
-	-	3
-	-	4
-	-	5
-	-	6
-	-	7
-	-	8
-	-	9
-	-	10
18	1	11
19	2	12
20	3	13
21	4	14
22	5	15
23	6	16
24	7	17
25	8	18
26	9	19
27	10	20
28	11	21
29	12	22
30	13	23
31	14	24
32	15	25
33	16	26
34	17	27
35	18	28
36	19	29
37	20	30
38	21	31
39	22	32
40	23	33
41	24	34
42	25	35
43	26	36
44	27	37
45	28	38
46	29	39
47	30	40
48	31	41
49	32	42
50	33	43
51	34	44
52	35	45
53	36	46
54	37	47
55	38	48
56	39	49
57	40	50
58	41	51
59	42	52
60	43	53
61	44	54
62	45	-
63	46	55
64	47	56
65	48	57
66	49	58
67	50	59
68	51	60
-	-	-
-	-	-
-	-	-
-	-	-
-	-	-
69	52	61
70	53	62
71	54	63
72	55	64
73	56	65
74	57	66
75	58	67
77	60	69
78	61	70
79	62	71
80	63	72
81	64	73
82	65	74
83	66	75
84	67	76
85	68	77
86	69	78
87	70	79
88	71	80
89	72	81
90	73	82
91	74	-
92	75	83
93	76	84
94	77	85
95	78	86
96	79	87
97	80	88
98	81	89
99	82	90
100	83	91
101	84	92
102	85	-
103	86	93
104	87	94
105	88	95
106	89	96
107	90	97
108	91	98
109	92	99
110	93	100
111	94	101
112	95	102
-	-	-
-	-	-
113	96	103
114	97	104
115	98	105
116	99	106
117	100	107
118	101	108
119	102	109
120	103	110
121	104	111
122	105	112
123	106	113
124	107	114
125	108	115
126	109	116
127	110	117
128	111	118
129	112	119
130	113	120
131	114	121
132	115	122
133	116	123
-	-	-
-	-	-
134	117	124
135	118	125
136	119	-
137	120	-
138	121	-
139	122	126
140	123	127
141	124	128
-	-	-
-	-	-
-	-	-
-	-	-
-	-	-
142	125	129
143	126	130
144	127	131
145	128	132
146	129	133
147	130	-
148	131	134
149	132	135
150	133	136
151	134	137
152	135	138
153	136	139
154	137	140
155	138	141
-	-	-
156	139	142
157	140	143
158	141	144
159	142	145
160	143	146
161	144	147
162	145	148
163	146	149
164	147	150
165	148	151
166	149	152
167	150	153
168	151	154
169	152	155
170	153	156
171	154	157
172	155	158
-	-	-
-	-	-
-	-	-
-	-	-
173	156	159
174	157	160
175	158	161
176	159	162
177	160	163
178	161	164
179	162	165
180	163	166
181	164	167
182	165	168
183	166	169
184	167	170
-	-	-
185	168	171
186	169	172
187	170	173
-	-	-
188	171	174
189	172	175
190	173	176
191	174	177
192	175	178
193	176	179
194	177	180
195	178	181
196	179	182
197	180	183
198	181	184
199	182	185
200	183	186
201	184	187
202	185	188
203	186	189
204	187	190
205	188	191
206	189	192
207	190	193
208	191	194
209	192	195
210	193	196
211	194	197
212	195	198
213	196	199
-	-	-
214	197	200
215	198	201
216	199	202
217	200	203
218	201	204
219	202	205
220	203	206
221	204	207
222	205	208
223	206	209
224	207	210
225	208	211
226	209	212
227	210	213
228	211	214
229	212	215
230	213	216
231	214	217
232	215	218
233	216	219
234	217	220
235	218	221
236	219	222
237	220	223
-	-	-
-	-	-
-	-	-
-	-	-
-	-	-
238	221	224
239	222	225
240	223	226
241	224	227
242	225	228
243	226	229
244	227	230
245	228	231
246	229	232
247	230	233
248	231	234
249	232	235
250	233	236
251	234	237
252	235	238
253	236	239
254	237	240
255	238	241
256	239	242
257	240	243
258	241	244
259	242	245
260	243	246
261	244	247
262	245	248
263	246	249
264	247	250
265	248	251
266	249	252
267	250	253
268	251	254
269	252	255
270	253	256
271	254	257
272	255	258
273	256	259
274	257	260
275	258	261
276	259	262
-	-	-
-	-	-
-	-	-
-	-	-
-	-	-
-	-	-
-	-	-
-	-	-
277	260	-
278	261	263
279	262	264
280	263	265
281	264	266
282	265	267
283	266	268
284	267	269
285	268	270
286	269	271
287	270	272
288	271	273
289	272	274
290	273	275
291	274	276
292	275	277
293	276	278
294	277	279
295	278	280
296	279	281
297	280	282
298	281	283
299	282	284
300	283	285
-	-	-
301	284	286
302	285	287
303	286	288
304	287	289
305	288	290
306	289	291
307	290	292
308	291	293
309	292	294
310	293	295
311	294	296
-	-	-
312	295	297
313	296	298